

See discussions, stats, and author profiles for this publication at: <http://www.researchgate.net/publication/267365440>

DYNAMIC INTERACTION OF RETAINING WALLS WITH RETAINED SOIL AND STRUCTURES

ARTICLE

READS

24

3 AUTHORS, INCLUDING:



[George Papazafeiropoulos](#)

National Technical University of Athens

7 PUBLICATIONS 4 CITATIONS

[SEE PROFILE](#)



[Yiannis Tsompanakis](#)

Technical University of Crete

65 PUBLICATIONS 357 CITATIONS

[SEE PROFILE](#)

DYNAMIC INTERACTION OF RETAINING WALLS WITH RETAINED SOIL AND STRUCTURES

Prodromos N. Psarropoulos¹, George Papazafeiropoulos², and Yiannis Tsompanakis²

¹ Hellenic Air-Force Academy, Greece
Department of Infrastructure Engineering
e-mail: prod@central.ntua.gr

² Technical University of Crete, Greece
Division of Mechanics, Department of Applied Sciences
gpapazafeiropoulos@yahoo.gr, jt@science.tuc.gr

Keywords: Dynamic interaction, soil impedance, dynamic distress, retaining walls.

Abstract. Retaining systems are widely used worldwide for serving various purposes in structures and infrastructures (embankments, bridges, ports, etc). The seismic response of various types of walls that support a single soil layer has been examined by a number of researchers in the past. Nevertheless, the dynamic interaction of the retaining walls with the structures that they are usually retained has not been investigated yet. It is evident, however, that during a seismic event the dynamic response of each component of this complex system (wall, soil, and superstructure) may affect substantially the response of the rest, and vice versa. The phenomenon of dynamic wall–soil–structure interaction (DWSSI) is a rather complicated issue that includes: (a) the dynamic interaction between a wall and a retained single soil layer, and (b) the “standard” dynamic soil–structure interaction (DSSI) of a structure with the underlying soil. In the present study, using numerical two-dimensional simulations, the influence of the wall characteristics (flexibility and smoothness) and its distance from the structure on the soil impedances (springs and dashpots) and on the distress of a cantilever wall are addressed. Emphasis is given on the variation of the soil impedance with the distance from the wall and with the exciting steady-state frequency. Subsequently, a structure founded on the retained soil is included in the numerical models, as a single-degree-of-system (SDOF). Despite the fact that there exist many open issues, the numerical results of the current study provide a clear indication of the direct dynamic interaction between a retaining wall and its retained structures. This justifies the necessity for a more elaborate consideration of these interrelated phenomena on the seismic design not only of the retaining walls but of the nearby structures as well, since the aforementioned dynamic interaction issues are not considered with adequate realism in the modern seismic norms.

1 INTRODUCTION

The main types of retaining systems are retaining walls supporting deep excavations, bridge abutments, and harbor-quay walls. In spite of the extensive use of retaining systems worldwide and their structural simplicity, the seismic response of such systems is a matter of ongoing research and has not yet been completely understood. The dynamic interaction between a wall and a retained soil layer increases the complexity of the problem, since material and/or geometry nonlinearities have to be taken into account [1,2]. The dynamic response of retaining walls has been examined by many researchers, experimentally, analytically, or numerically [3,4]. Depending on the expected material behavior of the retained soil and the possible mode of the wall displacement, there exist two main categories of analytical methods used in the design of retaining walls against earthquakes: (a) the *pseudo-static limiting-equilibrium* solutions which assume yielding walls resulting to plastic behavior of the retained soil [5,6,7], and (b) the *elasticity-based* solutions that consider the retained soil as a visco-elastic continuum [3,8,9].

An additional factor which complicates substantially the aforementioned dynamic interaction problem, is the presence of a structure (even of a simplified single-degree-of-freedom system) founded on the retained soil. It is evident that during a seismic event the dynamic response of each component of this complex system (wall, soil layer, foundation, structure) may affect substantially the response of the others. In other words, the presence of a retaining wall will affect not only the dynamic response of the structure but also its dynamic distress. Similarly, the presence of the structure may alter both the dynamic response and the dynamic earth pressures exerted on the wall. Thus, the phenomenon of *dynamic wall–soil–structure interaction (DWSSI)* is a rather complicated issue that includes: (a) the dynamic interaction between a wall and the retained soil layer, and (b) the “standard” dynamic soil–structure interaction (DSSI) of a structure with the underlying soil, via its foundation. The aforementioned dynamic interaction issues are considered in a simplistic way in the seismic norms currently used in engineering practice, like Eurocode 8 [10] or the Greek Seismic Code [11]. Regarding the design of retaining structures, the dynamic interaction between a retaining wall and the retained soil is ignored; while on the other hand, the issue of *dynamic soil–structure interaction* is considered a-priori to be beneficial for a structure, which seems not to be always the case [12].

Each of the two major components of the DWSSI, the DWSI and the DSSI, is comprised of two mechanisms which affect every kind of dynamic interaction: (a) the kinematic interaction, and (b) the inertial interaction. In the first case, the foundation of the structure is so stiff, that it cannot follow the free-field deformation of the underlying soil, namely the deformation which would occur without the presence of the structure. Pure kinematic soil–foundation interaction exists only when the whole structure is massless, and occurs if the foundation stiffness impedes the development of free-field motions [1]. In the latter case, the whole structure has non-zero mass and would respond dynamically (i.e., it has a non-zero finite eigenperiod), even if the underlying soil has infinite stiffness. If the soil is compliant, the whole problem (described as DSSI) is governed by inertial interaction. In this study, for the evaluation of the soil springs and dashpots, a rigid, massless foundation is considered, thus, the interaction is purely kinematic. As far as the calculation of the wall’s dynamic distress is concerned, the structure near the wall has a finite eigenfrequency greater than zero; hence, there exists inertial interaction.

The most common type of structure employed for a simplified analysis of inertial interaction, presented in Figure 1, is a single degree of freedom (SDOF) system which has height h and is founded on a flexible foundation medium represented by the frequency dependent and (complex-valued) translational and rotational springs and dashpots shown in the same figure.

This simple structure can be viewed as a model of a single-story building or, more generally, as an approximate model of a multistory building that is dominated by its fundamental mode response. In the latter case, h is interpreted as the height of the centroid of the inertial forces associated with the fundamental mode.

In the present study, given that two-dimensional plane-strain conditions are considered, the foundation is actually a strip with length much larger than its width. Simple formulas are provided in the literature, which can be used in order to calculate the stiffness and damping constants of the aforementioned springs and dashpots for foundations lying over a soil layer [13-20]. However, these empirical calculations are not valid, when a vertical boundary is placed near the foundation, which may be a retaining wall. Hence, the spring stiffness and dashpot coefficient of the same foundation will be different in the vicinity of a retaining wall, from the corresponding one-dimensional values. The current study examines the main characteristics of a rigid retaining wall that can influence the related soil impedance coefficients. Symbols K_x and C_x denote the translational spring and dashpot respectively, while K_r , C_r are the rotational spring and dashpot respectively, all of them at the base of the structure simulating the underlying soil (i.e., the presence of the above springs is equivalent to the presence of the underlying soil). In addition, K_{str} , ξ_{str} denote the flexural stiffness and critical damping ratio of the column respectively. The above parameters are schematically shown in Figure 1.

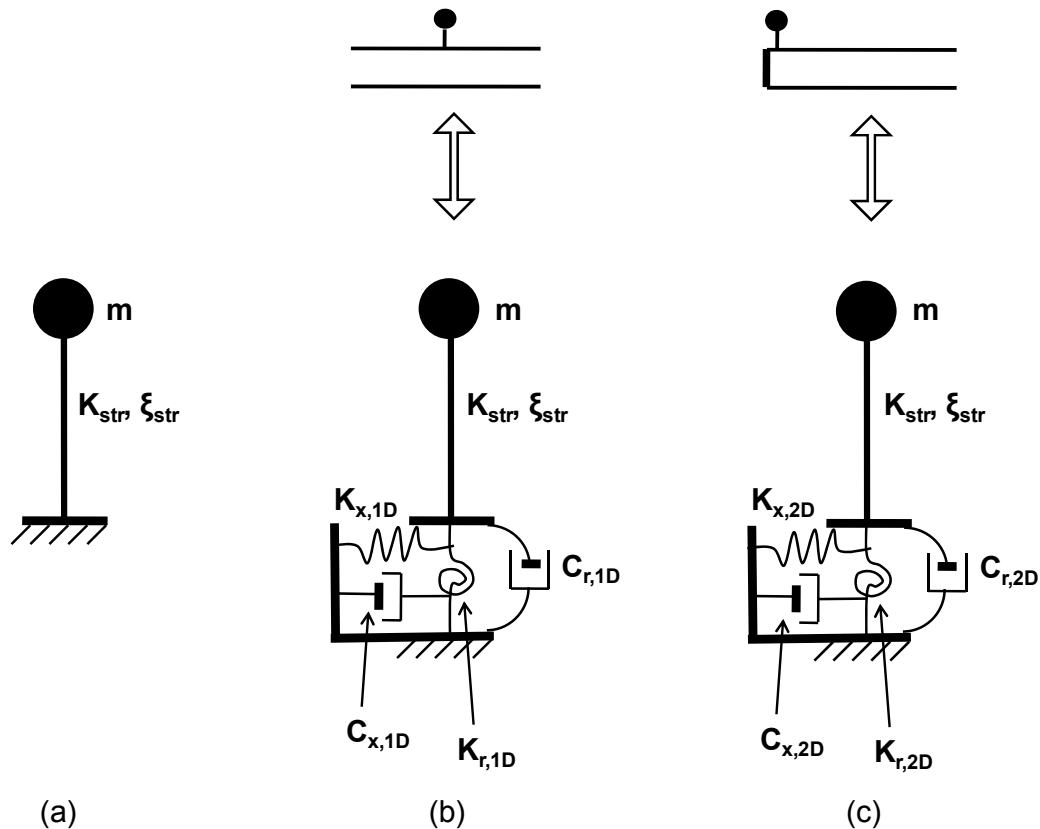


Figure 1: (a) A SDOF system lying on rigid rock, (b) the same SDOF system lying on an infinite deformable soil layer, and (c) the same SDOF system lying on a deformable soil layer, constrained by a retaining wall. Note that Figures 1b and 1c includes the equivalent springs and dashpots.

Apart from these considerations, the impact of an adjacent structure to the dynamic distress of the retaining wall is examined. It will be shown that the resultant thrust acting on the wall

originates mainly from the retained soil, while though the structure's influence is minor, it affects the local pressure distributions.

2 NUMERICAL MODELLING

The numerical models used in this study are intended to examine thoroughly all the factors which affect to a certain extent the dynamic response and distress of a retaining wall supporting an overlying structure. A semi-infinite soil layer of constant height H is considered, retained (or not) by a rigid or flexible wall. The flexibility of the wall is due to its flexural compliance as its base is totally fixed at the rigid rock which underlies the soil layer (Figure 2). Along the soil-rock interface horizontal and vertical fixity is assumed; the soil layer is free at its upper surface and it extends theoretically to infinity at the right side. Vertical kinematic constraints were used at that side of the model in order to simulate the one-dimensional soil layer response. The vertical kinematic constraints were placed far away from the wall in order to simulate the semi-infinite stratum more accurately. The length of the soil layer was selected to be 20 times its height, ensuring thus one-dimensional dynamic response in areas far away from the wall. The soil layer is characterized by its density γ , shear modulus G , Poisson's ratio ν , and critical damping ratio ζ . These properties are assumed to be constant all over the soil layer.

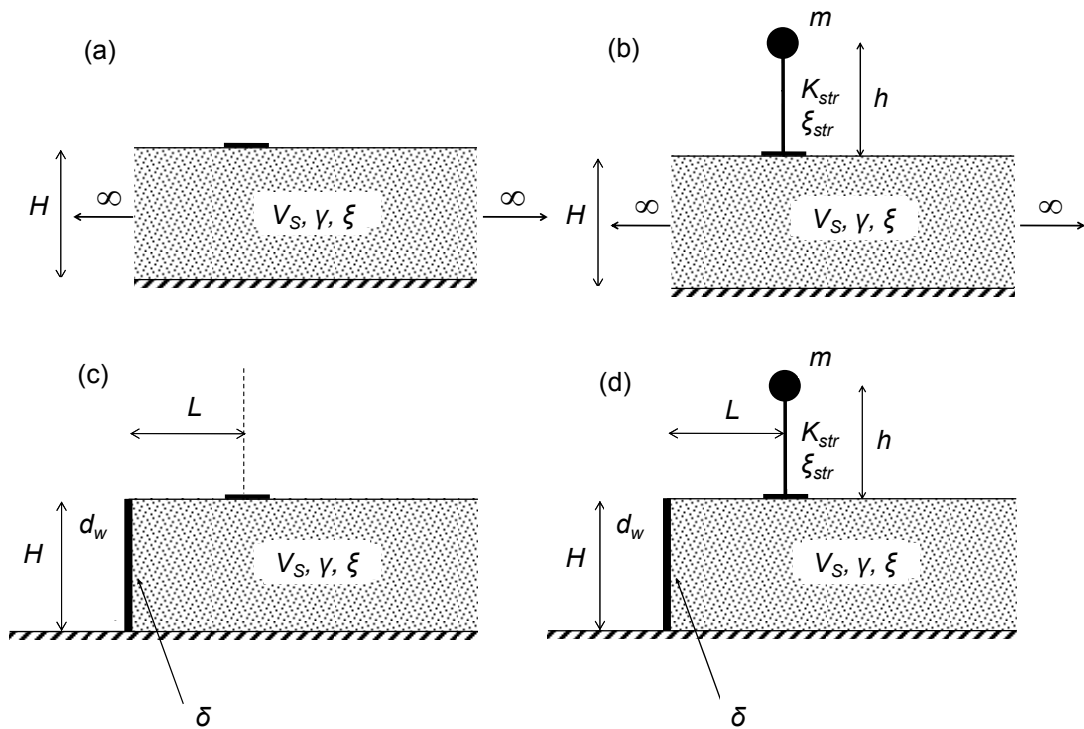


Figure 2: The four systems examined: (a) a rigid foundation lying on an infinite deformable soil layer, (b) a SDOF system founded on an infinite deformable soil layer, (c) a wall retaining a deformable soil layer on which a rigid foundation is lying at distance L , (d) a wall retaining a deformable soil layer on which a structure is founded at distance L .

On the surface of the soil layer a SDOF system is located, as shown in Figures 1 and 2. The column and foundation of the structure as well as the retaining wall are considered to be massless. Thus, inertial DWSI is avoided. Furthermore, the structure's foundation was consi-

dered to be rigid. The structure has, at the top of its column, a concentrated mass m , while the flexural stiffness of its column is K_{str} and its damping ratio equal to ζ_{str} . Its foundation is regarded to be in tied contact with the underlying soil, an assumption generally valid for cohesive soils. The position of the structure with respect to the retaining wall can be altered. By decreasing the above distance the contribution of the overlying structure to the wall distress becomes more significant, while a relatively large distance means that the wall responds independently of the structure. As far as the wall-soil interface is concerned two extreme cases were considered: (a) fully bonded wall-soil interface (which cannot slide, and corresponds to a large friction angle $\delta \gg 0$) and (b) smooth wall-soil interface (along which relative slippage can take place and corresponds to $\delta = 0$). Finally, a harmonic steady-state excitation is imposed on the system at the rigid rock.

In order to examine the effects of $DWSSI$ on both retaining wall and retained structures, two-dimensional (2-D) numerical simulations of the four retaining systems depicted in Figure 2 were conducted. The simulations were performed utilizing the finite-element code ABAQUS [21], which can perform linear dynamic analyses using Rayleigh material damping (which results from the sum of two components, one mass-proportional and one stiffness-proportional). The retained soil layer was discretized with 4-noded plane strain finite elements, while the SDOF column and the retaining wall were modeled using beam elements. For beams made from uniform material, shear flexible beam theory can provide useful results for cross-sectional dimensions up to 1/8 of a typical axial distance or the wavelength of the highest natural mode that contributes significantly to the response. Beyond this ratio the behavior of the member cannot be solely described as a function of axial position (i.e., Euler-Bernoulli beam theory). Thus, shear flexible beam elements were used in the numerical models. The beam elements of the wall have unit longitudinal dimension and thickness equal to $t_w = 0.20\text{m}$, whereas the beam elements of the structure's foundation and column have unit longitudinal dimension and thickness equal to $t = 0.60\text{m}$. The height of the SDOF was taken equal to 6m and the foundation's length 3.2m. The main parameters that have been examined are:

(a) The relative flexibility of the wall:

$$d_w = \frac{GH^3}{D_w} \quad (1)$$

where D_w denotes the flexural rigidity per unit of length of the wall given by:

$$D_w = \frac{E_w t_w^3}{12(1 - \nu_w^2)} \quad (2)$$

while two extreme values of relative wall flexibility were considered, $d_w = 0$ (rigid wall) and $d_w = 40$ (flexible wall). Given the value of d_w , the modulus of elasticity of the wall E_w is evaluated using Equations (1) and (2), while the Poisson's ratio ν_w is taken as 0.2.

(b) The distance of the column from the retaining wall L , normalized with respect to the height of the soil layer H , L/H . For $L/H > 10$ the retaining wall experiences practically no additional distress by the existence of the overlying structure. The minimum value of this ratio was considered equal to 0.3, since lower values would either cause numerical deficiencies, or could be infeasible due to the length of the foundation.

(c) The type of contact along the interface between the wall and the retained soil. This is expressed by the soil-wall friction angle δ . Two cases were considered in this study ($\delta \gg 0$)

and $\delta=0$) which correspond to bonded and smooth interface, respectively. By $\delta \gg 0$ it is implied that there is no relative sliding of the soil with respect to the wall and that the angle δ is large enough to avoid shear failure of the linearly responding soil along the interface.

(d) the frequency of the imposed harmonic excitation f , since a range of 0 to 8 Hz was considered, representing the typical frequency range of the majority of the seismic excitations. Steady-state analyses with sinusoidal excitations were performed which covered uniformly the above frequency band.

3 IMPACT OF DWSSI ON SOIL IMPEDANCE

Generally, a rigid foundation possesses six degrees of freedom in space (three translational and three rotational along x, y, z axis) and three degrees of freedom for two-dimensional conditions (two translational for x, y and one rotational for z). Given that an earthquake imposes primarily horizontal ground motion, only the horizontal and the rotational springs are the main parameters which will determine the dynamic distress of the wall. For each degree of freedom, a dynamic impedance associated with the soil properties and the geometrical characteristics of the foundation is defined, in a manner that if the underlying soil is substituted by a spring with complex stiffness constant equal to this impedance, then the dynamic response and distress of the structure would be identical to the initially calculated values.

The real part of the complex impedance K_i is called “dynamic stiffness” which reflects the stiffness and inertia effects of the soil; the imaginary part is the product of the circular frequency imposed by the harmonic excitation ω and the “dashpot coefficient” C_i . Thus, it can be stated that:

$$Z_i = K_i + i\omega C_i \quad (3)$$

where the subscript i signifies the degree of freedom. The complex impedance Z_i reflects the force to displacement ratio in each degree of freedom:

$$Z_i = \frac{P_i}{u_i} \quad (4)$$

Initially, in order to isolate the dynamic impact on the complex-numbered impedance, static conditions were assumed. In this case, Equation (3) reduces to the well-known real valued stiffness K_i for the quasi-static harmonic excitation. This stiffness does not include mass-dependent properties, given that the foundation is massless. Hereafter, the quasi-static translational stiffness will be denoted by K_x , whereas the rotational one by K_r . To further distinguish the one-dimensional soil layer from the two-dimensional conditions, the symbols $K_{x,1D}$, $K_{r,1D}$, $K_{x,2D}$, and $K_{r,2D}$ are used. The subscript 1D indicates that underlying soil layer extends to infinity at both directions, and 2D denotes the presence of an adjacent wall, which makes the model actually two-dimensional. In the two-dimensional case, if not explicitly mentioned, it is considered that the normalized distance L/H of the structure is equal to 0.3. The stiffnesses $K_{x,1D}$, $K_{r,1D}$, are given by the relations:

$$K_{x,1D} \approx \frac{2.1G}{2-\nu} \left(1 + \frac{2B}{H} \right) \quad (5)$$

$$K_{r,1D} \approx \frac{\pi GB^2}{2(1-\nu)} \left(1 + \frac{B}{5H} \right) \quad (6)$$

3.1 Impact of the frequency content

The dynamic response of the whole wall-soil-SDOF (WSS) system depends mainly on the characteristics of the imposed excitation (both in the time and frequency domain). In addition, it is possible to decompose every arbitrary seismic excitation into a number of sinusoidal pulses, with selected amplitudes and frequencies (Fast Fourier Transform). Therefore, the impact of a harmonic excitation on the various parameters of the retained soil impedance is examined for rigid strip foundations in the vicinity of the retaining wall.

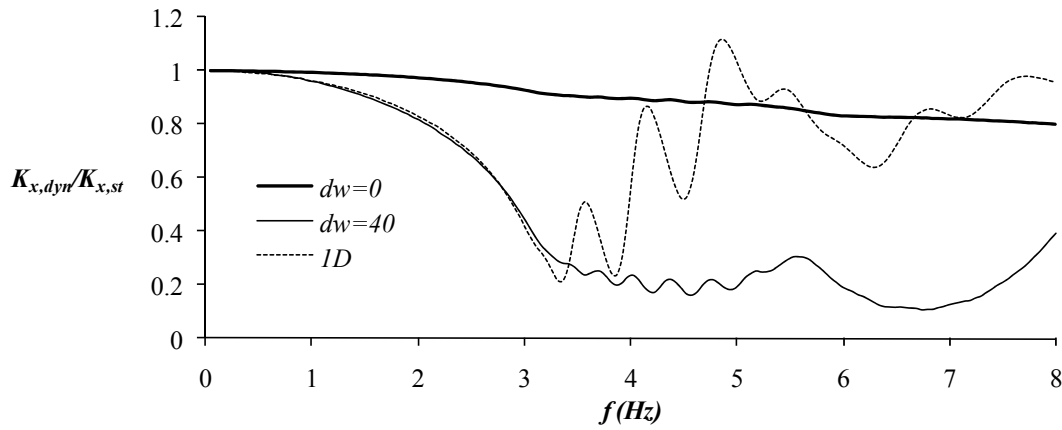


Figure 3: Dynamic horizontal stiffness to static horizontal stiffness ratio versus the frequency of the imposed harmonic excitation, in the vicinity of a rigid wall ($d_w=0$), a flexible wall ($d_w=40$) and for free-field conditions at an infinite distance from the wall (1D).

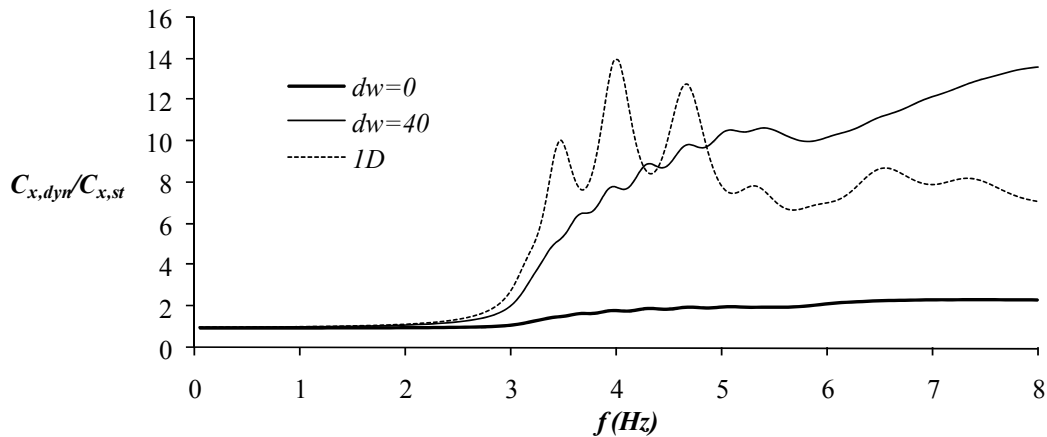


Figure 4: Dynamic horizontal dashpot coefficient to static horizontal dashpot coefficient ratio versus the frequency of the imposed harmonic excitation, in the vicinity of a rigid wall ($d_w=0$), a flexible wall ($d_w=40$) and for free-field conditions at an infinite distance from the wall (1D).

Figure 3 shows the dynamic horizontal stiffness normalized with the static horizontal stiffness $K_{x,dyn}/K_{x,st}$ versus the excitation frequency f , for the two extreme cases of wall flexibility compared to the case in which the soil responds one-dimensionally way. Generally, all stiffness constants, except for the case of rigid wall, seem to decrease in relation to the static values, if dynamic loading is considered.

Figure 4 shows the dynamic horizontal dashpot coefficient normalized to the static horizontal dashpot coefficient $C_{x,dyn}/C_{x,st}$ for the same cases as above. Contrary to their stiffness counterparts, the curves demonstrate an increase of the dashpot coefficients compared to their static values in dynamic conditions, which can be as much as fourteen times their static value. Once more, the rigid wall case gives substantially different trends. In both Figures 3 and 4 a number of undulations are shown, which become more intense in the case of 1D soil response. The crests and troughs shown in the case of flexible wall ($d_w=40$) are much more smoother than those for the rigid wall with a constant tendency to increase. Notice that these fluctuations are minimized in the case of rigid wall ($d_w=0$). Hence, they have to be attributed to reflected waves from the rigid rock under the soil layer.

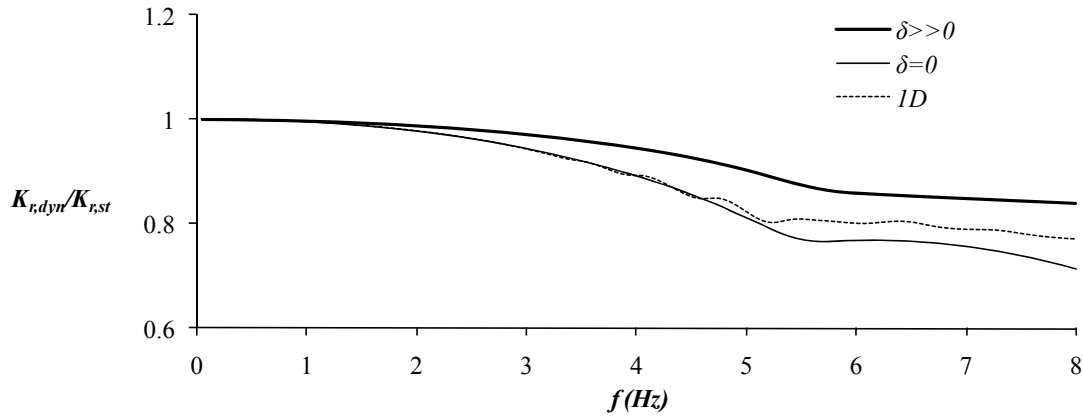


Figure 5: Dynamic rotational stiffness to static rotational stiffness ratio versus the frequency of the imposed harmonic excitation, in the vicinity of a rough wall ($\delta \gg 0$), a smooth wall ($\delta=0$) and for free-field conditions at an infinite distance from the wall (1D).

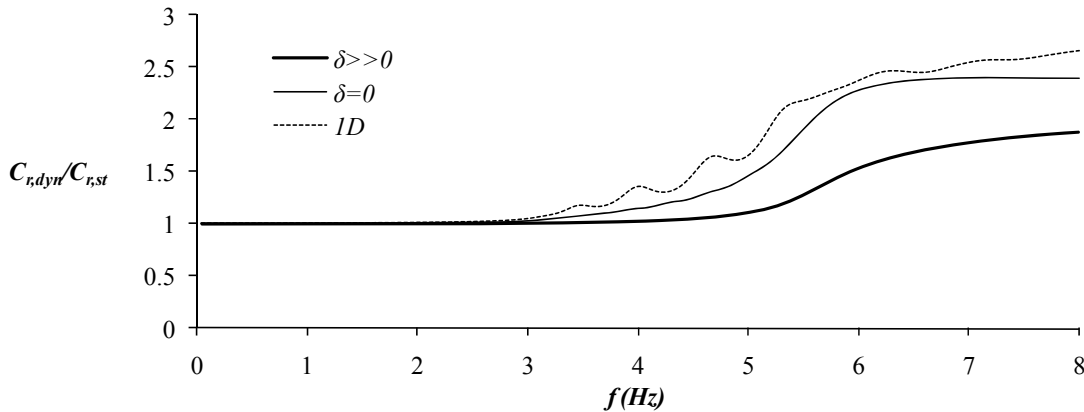


Figure 6: Dynamic rotational dashpot coefficient to static rotational dashpot coefficient ratio versus the frequency of the imposed harmonic excitation, in the vicinity of a rough wall ($\delta \gg 0$), a smooth wall ($\delta=0$) and for free-field conditions at an infinite distance from the wall (1D).

Generally, the same trends are observed for the rotational stiffness and dashpot coefficient, plotted in Figures 5 and 6 respectively, for three cases: one for bonded wall-soil interface ($\delta \gg 0$), one for smooth wall-soil interface ($\delta = 0$) and finally one for 1D soil response. In the case of 1D response, the rotational stiffness seems to take intermediate values between the two extreme cases of wall flexibility. This is not the case for the rotational dashpot coefficient. Moreover, the rotational constants do not show as large fluctuations as the horizontal ones shown in Figures 3 and 4. Generally, dynamic response has a decreasing effect on stiffness and an increasing effect on damping, as the previous figures have presented.

3.2 Impact of the SDOF distance from the wall

Figure 7 depicts the variation of the ratio of the static translational stiffness coefficients, ($K_{x,2D}/K_{x,1D}$) versus the dimensionless distance of the structure from the wall L/H , for two different cases of retaining wall compliance: $d_w=0$ (rigid) and $d_w=40$ (flexible). The wall-soil interface is considered to be bonded. These diagrams provide useful information about the effects of an adjacent retaining wall to the soil translational static stiffness. The static stiffness may either increase so that it becomes nearly double, or decrease even by 25 % with respect to the corresponding 1D value, which depends on the wall's flexibility.

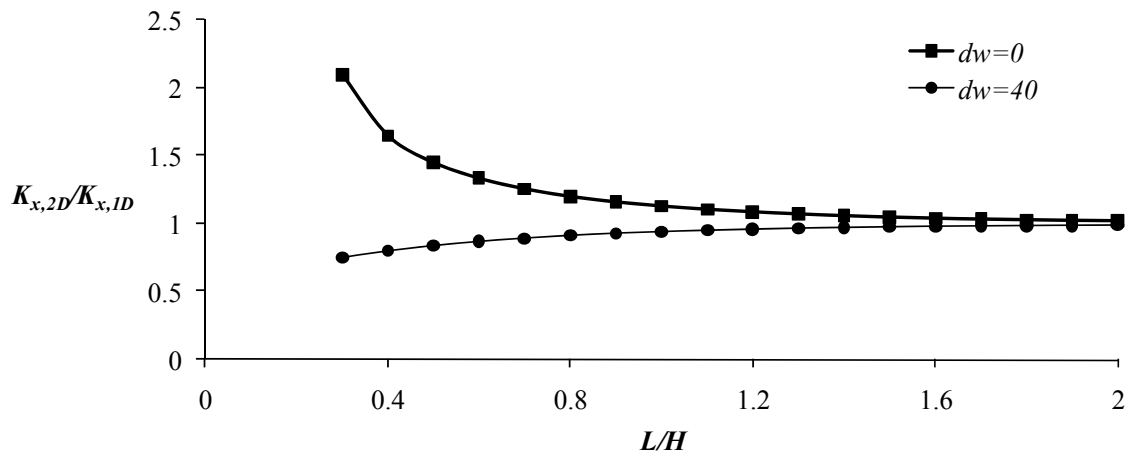


Figure 7: Static translational stiffness behind a retaining wall to static translational stiffness in 1D conditions ratio versus the dimensionless distance from the wall L/H , for a rigid retaining wall ($d_w=0$) and a flexible retaining wall ($d_w=40$).

In Figure 8 the corresponding diagram for the rotational stiffness ($K_{r,2D}/K_{r,1D}$) is shown. It can be observed that the wall flexibility has nearly no effect on the static rotational stiffness of the soil. A possible explanation for this is that the wall flexibility has influence mainly in the horizontal direction, even if the soil-wall interface is fully bonded. Apart from that, the rotation of an initially horizontal foundation induces only vertical displacements at its ends. Contrary to the relative wall flexibility d_w , the soil-wall interface friction angle δ is supposed to have a non-trivial effect on the rotational stiffness as this interface is a vertical boundary, which will affect only the vertical displacements of the footing. According to an elaborate investigation that was performed in this work, the horizontal stiffness of the underlying soil seems to be insensitive to the wall-soil friction angle δ .

Contrary to the retaining wall compliance, the aforementioned wall-soil friction angle seems to be a crucial factor for the rotational soil stiffness as illustrated in Figure 9. In the

case of smooth interface ($\delta=0$) and as the structure approaches the wall, the rotational stiffness decreasing (by approximately 20%), while the latter increases up to the same percentage, if the interface is bonded ($\delta \gg 0$). As long as the soil exhibits linear elastic behavior, its static rotational stiffness ratio ($K_{x,2D}/K_{x,1D}$) is a function of the relative flexibility of the wall d_w and the dimensionless distance L/H . Similarly, the static rotational stiffness ratio ($K_{r,2D}/K_{r,1D}$) is a function of the wall-soil friction angle δ and the dimensionless distance L/H .

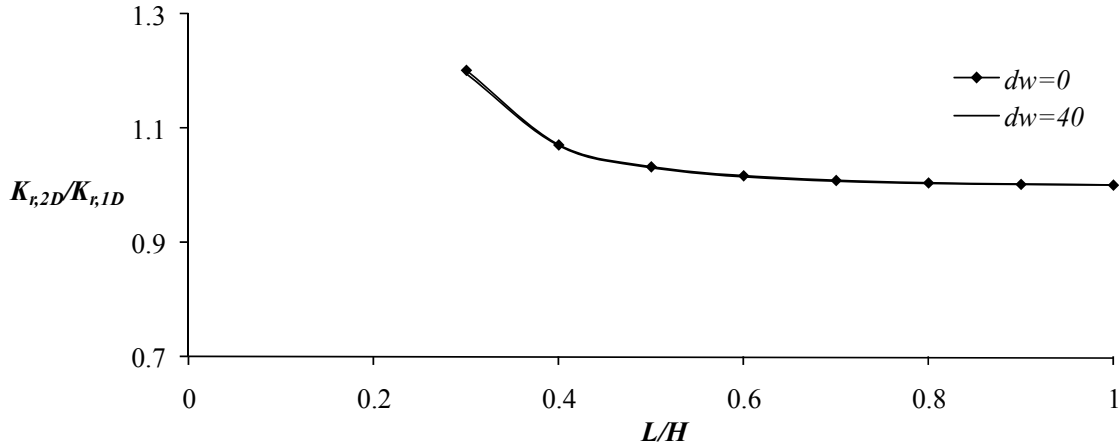


Figure 8: Static rotational stiffness behind a retaining wall to static rotational stiffness in 1D conditions ratio versus the dimensionless distance from the wall L/H , for a rigid retaining wall ($d_w=0$) and a flexible retaining wall ($d_w=40$).

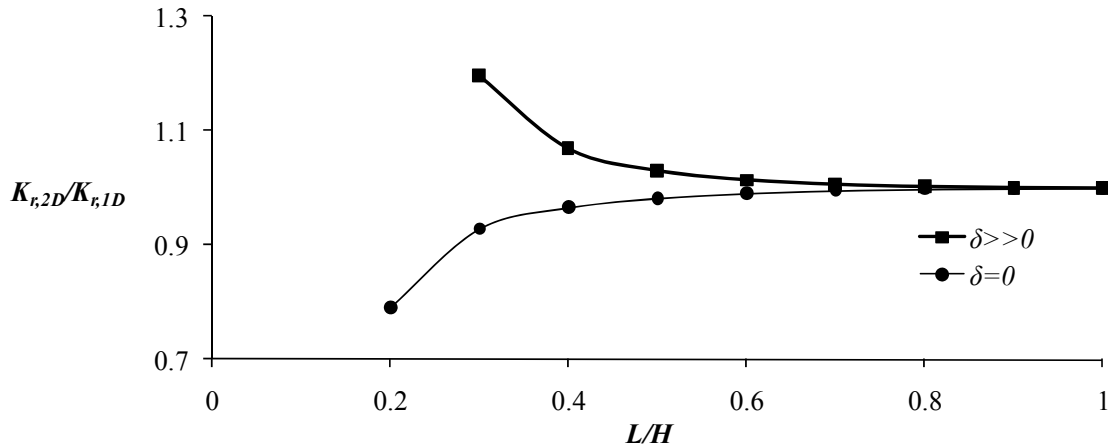


Figure 9: Static rotational stiffness behind a retaining wall to static rotational stiffness in 1D conditions ratio versus the dimensionless distance from the wall L/H , for a rough retaining wall ($\delta \gg 0$) and a smooth retaining wall ($\delta=0$).

Apart from quasi-static excitation, dynamic effects were also included in the equivalent soil stiffness and dashpot calculations. Figure 10 presents the dynamic translational stiffness ratio ($K_{x,2D}/K_{x,1D}$) versus the frequency f of the imposed steady state harmonic excitation for the two examined cases of retaining wall, in which a bonded wall-soil interface is assumed. It is obvious that in the case of the rigid retaining wall the dynamic stiffness of the foundation of an adjacent structure may be as high as ten times the dynamic stiffness of the structure if it

was cited far away from the wall. This fact demonstrates that the wall acts in a beneficial way, by increasing the dynamic stiffness of the soil.

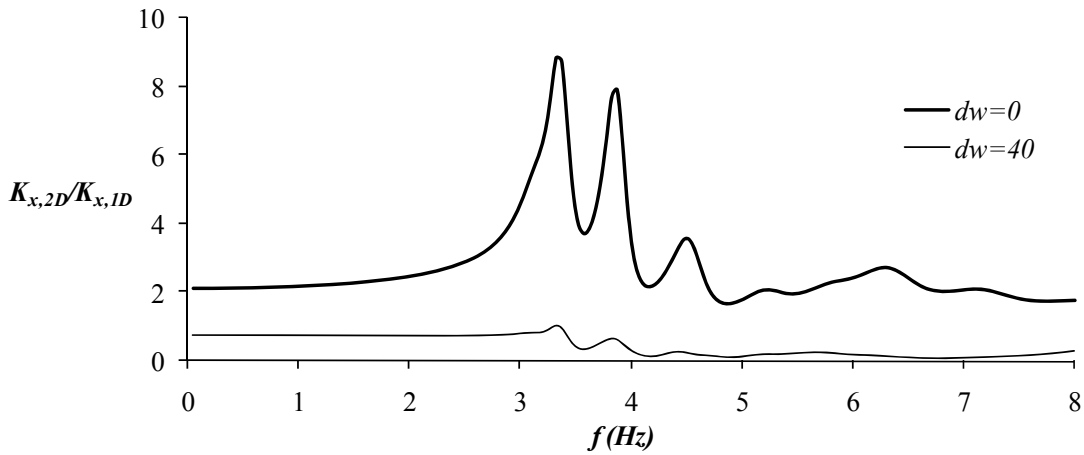


Figure 10: Ratio of dynamic translational stiffness behind a retaining wall to dynamic translational stiffness in 1D conditions versus the frequency of the imposed harmonic excitation for a rigid retaining wall ($d_w=0$) and a flexible retaining wall ($d_w=40$).

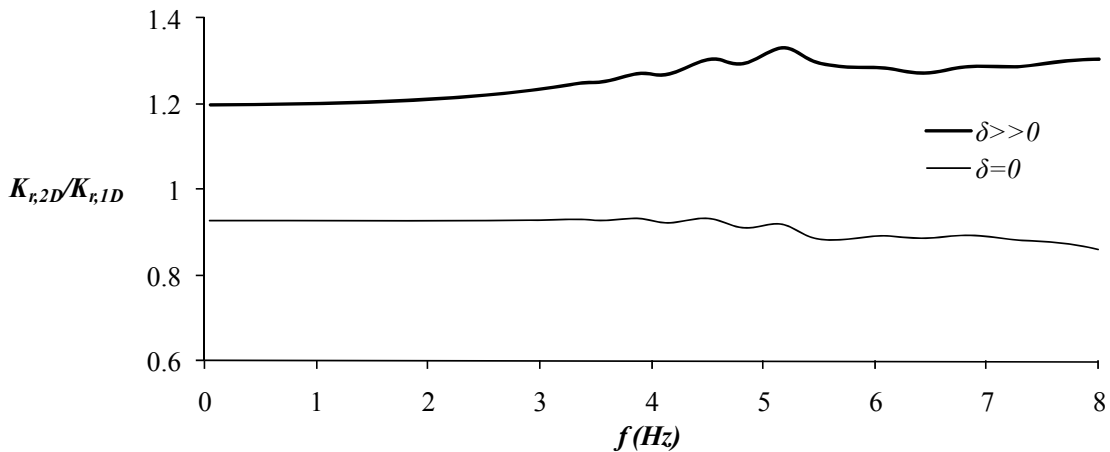


Figure 11: Ratio of dynamic rotational stiffness behind a retaining wall to dynamic rotational stiffness in 1D conditions versus the frequency of the imposed harmonic excitation for a rough retaining wall ($\delta \gg 0$) and a smooth retaining wall ($\delta=0$).

Local precipitous peaks for frequencies between 3 Hz and 4 Hz can be observed in Figure 10 for the case of $d_w=0$. However, the same does not happen in the case of the flexible wall. In the same figure it can be seen that the dynamic response of the rigid wall has a decreasing effect on the original dynamic stiffness of the soil for all the frequency range, which is typical for actual earthquakes. Especially at higher frequencies the value of $K_{x,2D}$ reaches 10% of the initial value $K_{x,1D}$. Therefore, engineers must be aware of this large reduction of $K_{x,2D}$, as in those cases the wall acts in a detrimental way and weakens the stability of the structure. In any case, Rayleigh damping may be increased at higher frequencies.

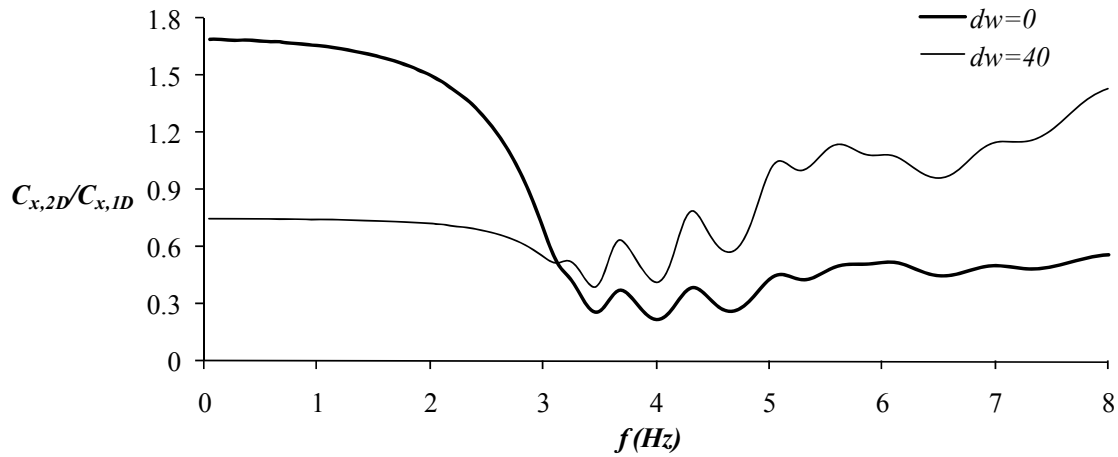


Figure 12: Ratio of dynamic translational dashpot coefficient behind a retaining wall to dynamic translational dashpot coefficient in 1D conditions versus the frequency of the imposed harmonic excitation for a rigid retaining wall ($d_w=0$) and a flexible retaining wall ($d_w=40$).

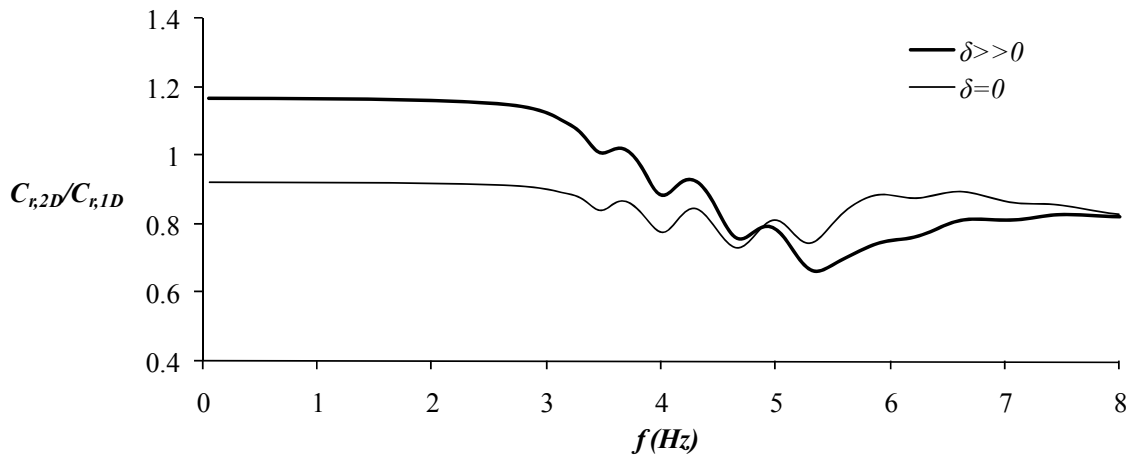


Figure 13: Ratio of dynamic rotational dashpot coefficient behind a retaining wall to dynamic rotational dashpot coefficient in 1D conditions versus the frequency of the imposed harmonic excitation for a rough retaining wall ($\delta \gg 0$) and a smooth retaining wall ($\delta=0$).

Figure 11 shows the dynamic stiffness $K_{r,2D}$ to $K_{r,1D}$ ratio versus the frequency of the imposed steady state harmonic excitation, for two cases of the wall-soil friction angle δ ($\delta=0$ and $\delta \gg 0$) for flexible wall case. The trend observed here is that the friction between the wall and the retained soil increases the dynamic stiffness of the soil by at least 20%. On the contrary, smoothness of the wall-soil interface renders the dynamic stiffness of the soil constantly lower than its initial value. These observations can be attributed to the fact that a bonded interface does not permit any relative slippage, thus, the soil cannot subside near the wall, a fact that explains the increased difficulty for the overlying foundation to rotate.

Apart from the dynamic stiffness the dashpot coefficients of the system were also studied. In Figure 12 the dynamic translational dashpot coefficient $C_{x,2D}$ to $C_{x,1D}$ ratio versus the frequency of the imposed steady state harmonic excitation, for two cases of retaining wall compliance is plotted. Bonded wall-soil interface is assumed. At low frequency levels, a rigid wall induces increased damping to the foundation, thus, more energy is absorbed. However, as the

frequency of the imposed excitation increases, the damping induced by the wall decreases, and it gets even lower from the dashpot coefficient which corresponds to 1D soil behavior. Moreover, the opposite trend is noticed for the flexible wall, which initially reduces damping and subsequently amplifies the dashpot coefficient values for frequencies higher than 5 Hz. Note that both curves exhibit more intense fluctuations (crests and troughs) in the frequency range approximately from 3 Hz to 5 Hz, which may happen due to wave reflections on the wall and the horizontal boundary imposed by the rigid rock on the soil layer.

Similarly, in Figure 13 the dashpot coefficient $C_{r,2D}$ to $C_{r,1D}$ ratio versus the frequency of the imposed steady state harmonic excitation is shown for two cases of the wall-soil friction angle δ ($\delta=0$ and $\delta \gg 0$), while the wall is considered flexible ($d_w=40$). A number of undulations is observed which are caused by wave reflections on the flexible wall. As expected, for zero wall-soil friction angle the influence of the wall presence is detrimental (the ratio is constantly lower than unity), whereas in the case of bonded wall-soil interface beneficial effects are noted for low frequencies up to 4 Hz.

Note that the frequencies where dashpot coefficient diagrams have local minima are almost equal to the frequencies where dynamic stiffness diagrams exhibit local maxima. Hence, it can be concluded that dynamic interaction induces an increasing effect on dynamic stiffness and a reducing effect on damping. Note also that the maxima of the two dynamic stiffness diagrams correspond to different frequencies and the same stands for the damping diagrams.

The “shearing” modes of the soil vibration (horizontal displacement) are controlled by the fundamental eigenfrequency of the soil layer which is:

$$f_{0,S} = \frac{V_s}{4H} \quad (7)$$

while for the compressing modes (rotation) the corresponding frequency is:

$$f_{0,P} = \frac{3.4}{\pi(1-\nu)} f_{0,S} \quad (8)$$

After substituting the soil data of the examined model in the two above equations it results that $f_{0,S} \approx 3.1$ Hz and $f_{0,P} \approx 4.8$ Hz. The former frequency is roughly the position of the maximum of the K_x and C_x diagrams and the latter is the position of the maximum of the K_r and C_r diagrams, as noted in Figures 10 to 13.

4 IMPACT OF DWSSI ON THE RETAINING WALL DISTRESS

Apart from the soil impedance, the additional distress of the retaining wall is investigated, due to the presence of the overlying structure. The wall and the structure’s foundation were considered rigid and massless. The SDOF column was considered to be massless and flexible. Two cases were examined: (a) there is not any structure at all, and (b) there exists a SDOF structure on the retained soil, which is located in a normalized distance from the wall equal to $L/H=0.3$. The modulus of elasticity of the SDOF column E was taken equal to 30GPa, its Poisson ratio $\nu=0.2$ (reinforced concrete) and the concentrated mass at its top equal to 4870 Kg. Rayleigh damping was also considered at the structure which results in 5% of critical damping at its fundamental eigenfrequency. It is also assumed that no de-bonding or relative slip happens along the wall-soil interface.

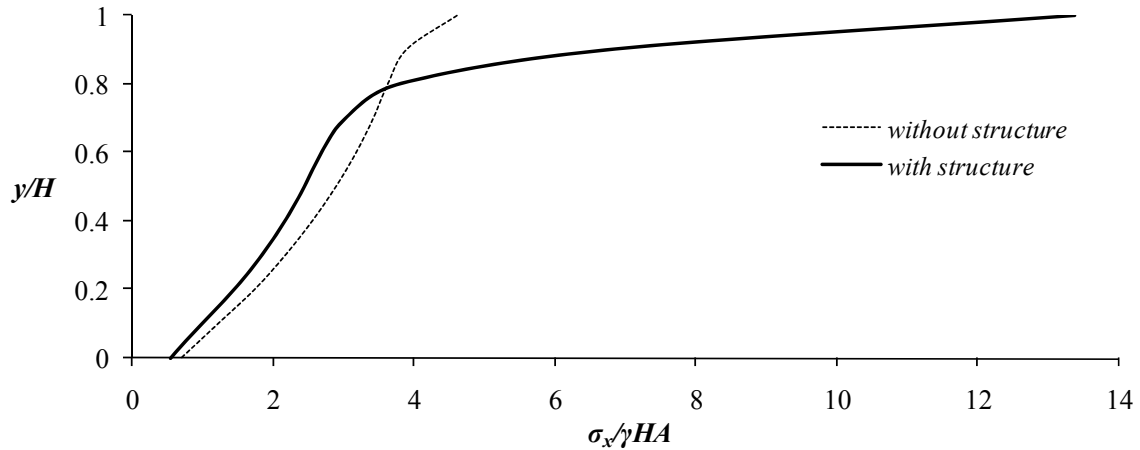


Figure 14: Normalized dynamic earth pressures plotted against the dimensionless height from the wall base, with and without an adjacent SDOF for the rigid wall case.

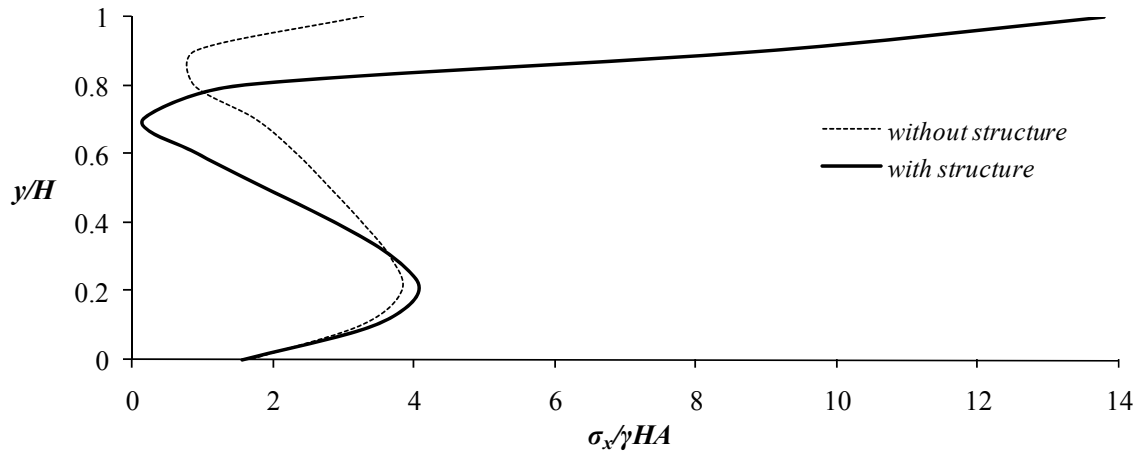


Figure 15: Normalized dynamic earth pressures plotted against the dimensionless height from the wall base, with and without an adjacent SDOF for the rigid wall case.

In general, the soil material properties (G , γ) and the wall height alone do not affect the dynamic pressures on the wall, as the wall flexibility is examined in relation to soil stiffness and the earth pressures are normalized with γ and H . Taking that point into account, all the analyses were performed considering an 8m-high wall. The retained soil layer is characterized by a relatively low shear-wave velocity V_S equal to 100m/s, a unit weight γ of 18kN/m³, Poisson's ratio $\nu=0.3$ and critical damping ratio $\zeta=5\%$ adjusted to the fundamental eigenfrequency $f_{0,S}$ of the soil layer.

Figure 14 depicts the normalized dynamic earth pressures induced by the soil to the rigid wall for both the two aforementioned cases (with and without a nearby SDOF), against the dimensionless height from the wall base. As expected, the horizontal normal stress (earth pressure) is larger if a structure exists near the wall. The normalized dynamic earth pressures in the case of the flexible wall are shown in Figure 15. Substantial differences are observed between Figures 14 and 15. The pressures are no longer positive (i.e., they become compress-

sive) if the wall is flexible. However, the pressures developed when a structure is present, are much larger in both cases.

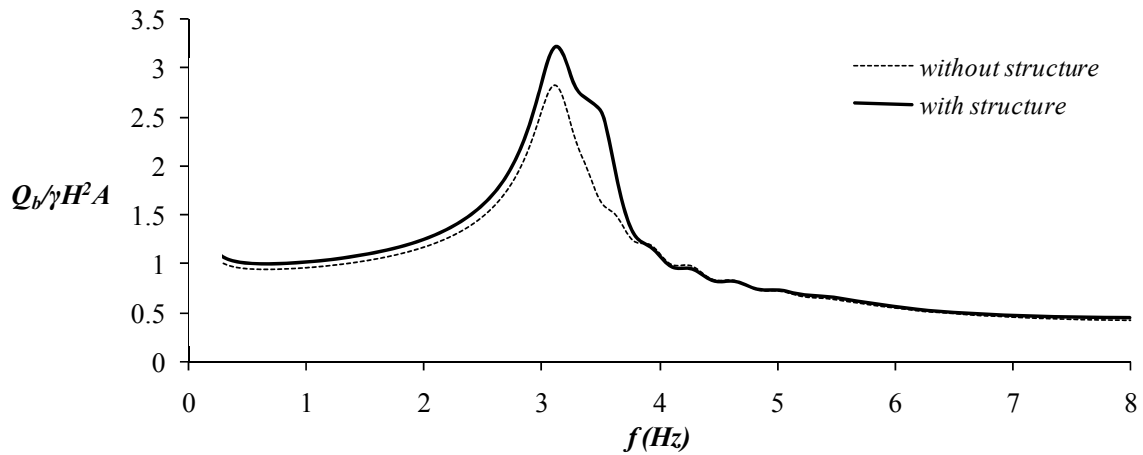


Figure 16: Normalized dynamic shear force at the base of a rigid wall plotted against the frequency of the imposed harmonic excitation with and without an adjacent SDOF.

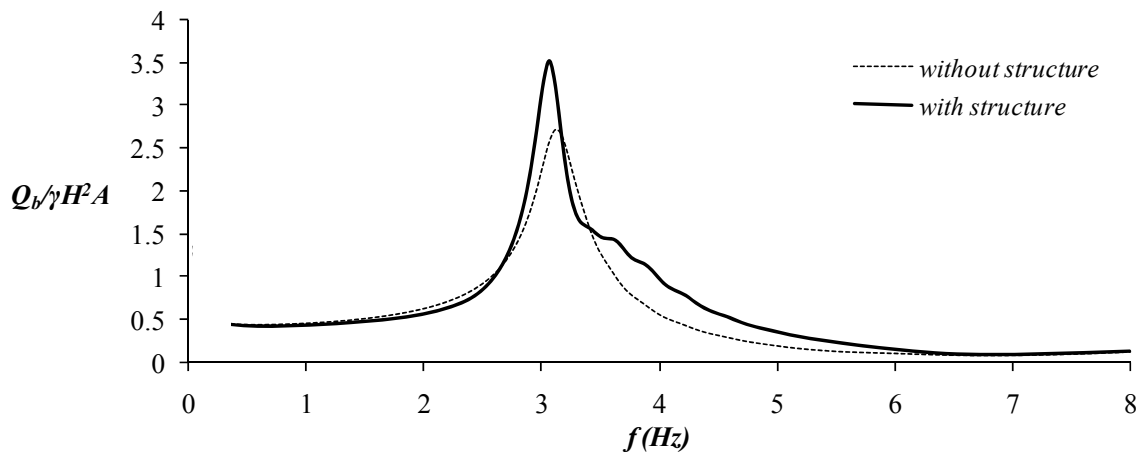


Figure 17: Normalized dynamic shear force at the base of a flexible wall plotted against the frequency of the imposed harmonic excitation with and without an adjacent SDOF.

If the dynamic earth pressures are integrated heightwise two derivative quantities will result that can describe the whole wall distress: the shear force and the bending moment at its base. In Figures 16 and 17 the dynamic shear force is plotted, against the frequency of the imposed harmonic excitation. The former figure presents the distress of a rigid wall, while the latter for a flexible wall. Despite the difference between the pairs of curves shown in the two plots, rather minor differences are observed in the resultant soil thrust when a SDOF structure is founded near the retaining wall's top. It seems that the increase in the distress of a flexible wall is larger (due to the structure's presence) than that of a rigid wall. The aforementioned trends are also observed for the bending moment, shown in Figures 18 and 19, where the increase due to the structure is higher and it becomes almost double in the case of the flexible wall (Figure 19). This fact can be attributed to the corresponding pressure distributions (Fig-

ures 14 and 15), which have their maximum value near the top of the wall, increasing thus the effective height of the resultant dynamic thrust.

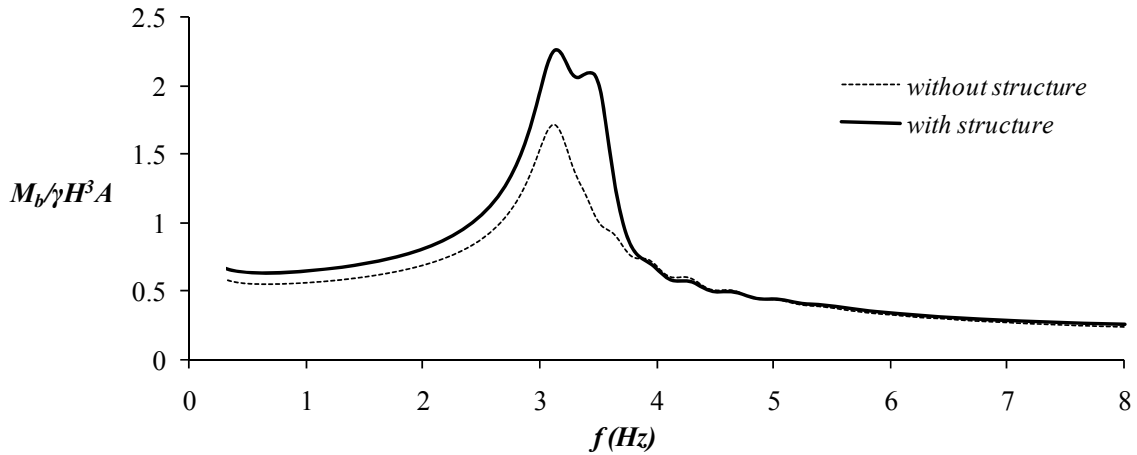


Figure 18: Normalized dynamic bending moment at the base of a rigid wall plotted against the frequency of the imposed harmonic excitation with and without an adjacent SDOF.

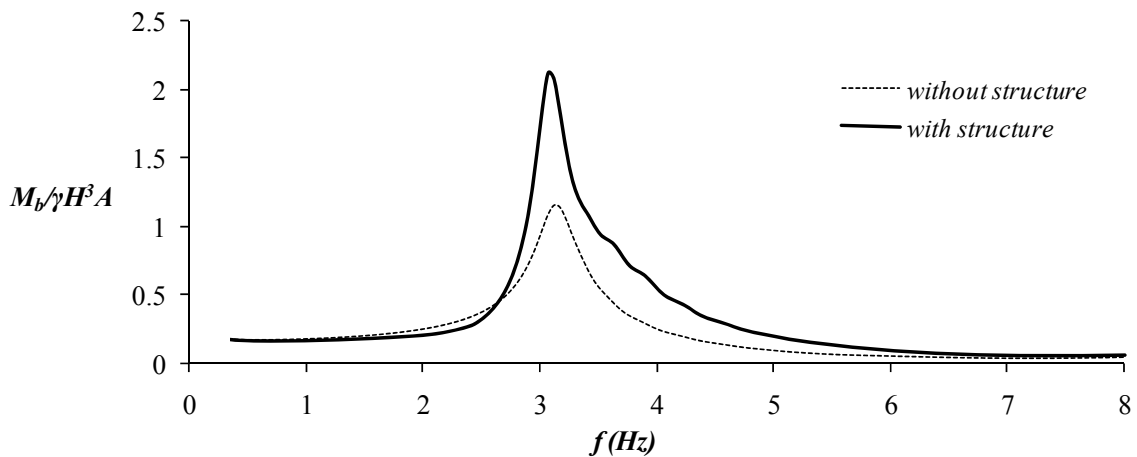


Figure 19: Normalized dynamic bending moment at the base of a flexible wall plotted against the frequency of the imposed harmonic excitation with and without an adjacent SDOF.

5 CONCLUSIONS

The complex dynamic wall–soil–structure interaction (DWSSI) phenomenon was investigated in this work, in terms of the foundation impedance and the retaining wall distress. One of the most important findings of the present study was that there is a clear dependence between the foundation impedance and the presence of a retaining wall adjacent to the structure. More specifically, the impact of the retaining wall presence can be described by using a number of dimensionless parameters. There is a significant impact of the normalized distance of the structure from the wall on the soil translational and rotational stiffness and dashpot coefficients. Furthermore, the rotational stiffness has proved to depend highly on the type of the wall-soil interface (bonded or smooth) and less on the flexural compliance of the retaining

wall. The opposite happens with the translational soil stiffness, which is affected primarily by the wall compliance and it is insensitive to variations of the wall-soil interface smoothness. The spring and dashpot curve configurations against frequency indicate the complexity of the DWSSI phenomenon in the frequency domain and highlight the necessity for a more elaborate consideration of the DWSSI effects.

Apart from the soil springs and dashpots, the dynamic earth pressures which develop on the cantilever retaining wall and the resultant soil thrust and bending moment were calculated. It was shown that, although the shear and normal pressure distributions differ substantially if there exists an overlying structure, since then the resultant shear force and bending moment at the wall base become slightly greater. The numerical results of the current study provide a clear indication of the direct dynamic interaction between a retaining wall and its retained structures. This justifies the necessity for a more elaborate consideration of this interrelated phenomenon on the seismic design, not only of the retaining walls but of the nearby structures as well.

REFERENCES

- [1] S. Kramer, *Geotechnical Earthquake Engineering*, Prentice Hall, 1996.
- [2] G. Wu and W.D.L. Finn, Seismic lateral pressures for design of rigid walls, *Canadian Geotechnical Journal* 36(3), 509-522, 1999.
- [3] A.S. Veletsos and A.H. Younan, Dynamic Response of Cantilever Retaining Walls, *ASCE Journal of Geotechnical and Geoenvironmental Engineering* 123(2), 161–172, 1997.
- [4] P.N. Psarropoulos, G. Klonaris, and G. Gazetas, Seismic earth pressures on rigid and flexible retaining walls, *Soil Dynamics and Earthquake Engineering* 25(7-10), 795-809, 2005.
- [5] S. Okabe, General theory of earth pressures, *Journal of the Japan Society of Civil Engineering*, 12(1), 1926.
- [6] N. Mononobe, and H. Matsuo, On the determination of earth pressures during earthquakes, Proceedings of the World Engineering Congress, Tokyo, Japan, Vol. 9, Paper 388, 1929.
- [7] H.B. Seed and R.V. Whitman, Design of earth retaining structures for dynamic loads, Proceedings of the ASCE Special Conference on Lateral Stresses in the Ground and Design of Earth Retaining Structures, pp. 103–147, 1970.
- [8] R.F. Scott, Earthquake-induced pressures on retaining walls, Proceedings of the 5th World Conference on Earthquake Engineering, Vol. 2, pp. 1611–1620, 1973.
- [9] J.H. Wood, Earthquake – Induced Pressures on a Rigid Wall Structure, *Bulletin of New Zealand National Earthquake Engineering* 8, 175–186, 1975.
- [10] EC8, Eurocode 8: Design of structures for earthquake resistance, European standard CEN-ENV-1998-1, European Committee for Standardization, Brussels, 2004.
- [11] EAK, Greek Seismic Code, Ministry of Public Works, Athens, Greece, 2000.
- [12] G. Mylonakis and G. Gazetas, Seismic soil-structure interaction: beneficial or detrimental?, *Journal of Earthquake Engineering* 4(3), 277-301, 2000.
- [13] G. Gazetas, *Foundation vibrations, Foundation Engineering Handbook*, 2nd edition, 1991.
- [14] G. Gazetas, Analysis of machine foundation vibrations: state of the art, *Soil Dynamics and Earthquake Engineering*, Vol. 2, No. 1, 1983.

- [15] R. Dobry and G. Gazetas, Dynamic Response of Arbitrarily Shaped Machine Foundations, *Journal of Geotechnical Engineering ASCE*, 112(2), 1986.
- [16] J. Dominguez and J.M. Roesset, Dynamic Stiffness of Rectangular Foundations, Research Report R78-20, Dept. of Civ. Engrg., MIT, 1978.
- [17] J.E. Luco, Linear soil-structure interaction, Soil-structure interaction: The status of current analysis methods and research, J. J. Johnson, ed., Rep. No. NUREG/CR-1780 and UCRL-53011, U.S. Nuclear Regulatory Commission, Washington, D.C. and Lawrence Livermore Laboratory, Livermore, CA, 1980.
- [18] J.M. Roesset, A review of soil-structure interaction, Soilstructure interaction: The status of current analysis methods and research, J. J. Johnson, ed., Rep. No. NUREG/CR-1780 and UCRL- 53011, U.S. Nuclear Regulatory Commission, Washington, D.C. and Lawrence Livermore Laboratory, Washington, D.C., 1980.
- [19] A.S. Veletsos and J.W. Meek, Dynamic behaviour of building-foundation systems, *Earthquake Engineering and Structural Dynamics*, 3, 121-138, 1974
- [20] J.P. Stewart, G.L. Fenves and R.B. Seed, Seismic soil–structure interaction in buildings I: Analytical methods, *Journal of Geotechnical and Geoenvironmental Engineering*, 125(1), 26–37, 1999.
- [21] ABAQUS, Analysis User’s Manual Version 6.4, ABAQUS Inc., USA, 2003.